# SINIFANÁ METASEDIMENTITES AND RELATIONS WITH CAJAMARCA PARAGNEISSES OF THE CENTRAL CORDILLERA OF COLOMBIA

# RELACIONES GEOLÓGICAS DE LAS METASEDIMENTITAS DE LA SINIFANÁ CON LOS PARANEISES DEL COMPLEJO CAJAMARCA DE LA CORDILLERA CENTRAL

UWE C. MARTENS

*Ph.D., Tectonic Analysis Inc. umartens@zoho.com*

JORGE JULIÁN RESTREPO

*MSc., Universidad Nacional de Colombia.*

LUIGI A. SOLARI

*Ph.D., Universidad Nacional Autónoma de México.*

Recibido para evaluación: 30 Octubre 2012/Aceptación: 15 Noviembre: 2012 / Recibida Versión Final: 29 Noviembre 2012

**ABSTRACT:** The western flank of Colombia's Central Cordillera is characterized by N-S elongated tectonic blocks within the continental-scale Romeral and Cauca fault system. One of these blocks comprises the slates, metasandstones and quartzites of the Sinifaná Metasedimentites along with the intrusive Amagá granitic Stock. Zircon U-Pb detrital geochronology was conducted on a Sinifaná metaquartzite taken ca. 40 km southwest of Medellin. The main population yielded 640–500 Ma ages, typical of the Pan African-Brasiliano event and suggestive of Gondwanan provenance. The sample also yielded minor Proterozoic ages and the three youngest detrital zircons yielded 325–290 Ma ages. Taking into account the intrusive but unmetamorphosed character of the ca. 230 Ma Amagá Stock, we conclude that deposition of Sinifaná terrigenous rocks and their metamorphism occurred between the late Carboniferous and earliest Triassic.

Sinifaná detrital-zircon populations are analogous to inherited zircon in Cajamarca migmatites and paragneisses from Las Palmas, near Medellin, which constitute the basement of the Tahamí terrane. This feature suggests a link between these high-grade metasedimentary rocks and the low grade metasedimentary rocks of the relatively small Sinifaná block. Metamorphic rims yielding 220–250 Ma, which are ubiquitous in Las Palmas, are absent in Sinifaná, probably due to very-low-grade metamorphism not producing zircon recrystallization. We propose that the tectonic block containing the Sinifaná metasedimentites may have broken away from a continental margin that once included both the Tahamí and other smaller pieces such as the Sinifaná. The age of tectonic departure is constrained by the block comprising the early Cretaceous Quebradagrande complex, which is currently positioned between the Tahamí and Sinifaná.

**Key Words:** U-Pb geochronology, Detrital zircons, Tahamí terrane, Margin Segmentation.

**RESUMEN:** El flanco occidental de la Cordillera Central Colombiana esta caracterizado por el presencia de bloques tectónicos elongados en el sentido N-S que se encuentran limitados por las fallas de Romercal y Cauca. Las pizarras, meta-arenitas y cuarcitas asociados a los Metasedimentos de la Sinifaná intruidas por el Stock de Amagá constituyen uno de estos bloques. Nuevos resultados de U-Pb en circones detríticos fueron obtenidos en una metacuarcita de asociada a los metasedimentos y expuesta a ca. 40 Km al suroeste de Medellín.

La principal población de circones presenta edades Panafricanas-Brasilianas (640-550 Ma) que indican una afinidad Gondwanica. Poblaciones definidas con menos granos presenan edades Proterozoicas, mientras que los tres granos más jóvenes reportan igualmente edades entre 325–290 Ma. Las relaciones intrusivas con las rocas no deformadas del Stock de Amagá que presenta edades de cristalización de 230 Ma sugieren que el metamorfismo ocurrió entre el Carbonífero tardío y el Triásico temprano.

Las poblaciones detríticas presentes en los Metasedimentos de la Sinifaná son semejantes a aquellas presentes en las migmatitas y paraneises de las Palmas con asociados al Complejo Cajamarca y que representan el basamento del terreno Tahamí. Estas semejanzas sugieren que ambas unidades estarán relacionados geológicamente y la ausencia de los sobrecrecimientos metamórficos entre 220 Ma y 250 Ma presentes en las Palmas estaría relacionado con el bajo grado de metamorfismo de las rocas de la Sinifaná.

Se sugiere que el bloque tectónico que contiene los Metasedimentos de la Sinifaná estaría relacionado al Terreno Tahamí y que habría sido segmentado durante el Cretácico como lo sugiere la ubicación de las rocas del Complejo Quebradagrande entre el Terreno Tahamí y los Metasedimentos de la Sinifaná.

**Palabras claves:** Geocronología U-Pb, Circones detríticos, Terreno Tahamí, Segmentación de la margen.

Boletín Ciencias de la Tierra, Nro. 32, pp. 99-110. Medellín, diciembre de 2012. ISSN 012-3630

## 1. INTRODUCTION

The Cauca-Romeral fault zone is an NS-elongated, continental-scale system that serves as the main boundary between terranes of oceanic and continental affinity in the northwestern Andes (Colombia and Ecuador). In northcentral Colombia, the fault system runs roughly along the boundary region between the Western and Central Cordilleras following the Cauca River. Within the fault system, a series of individual blocks and slivers of diverse origin has been identified (Figure 1). These include pieces of oceanic crust, oceanic plateau, island arcs, continental arc, medium-grade metamorphic units, among others. Establishing the relations between blocks and the larger terranes in the Colombian Andes is a critical task to reconstruct the geologic history of the northwestern Andes. This is accomplished by careful characterization of each of the blocks and assessment of their potential relations.

In this contribution we focus on the block comprising the Sinifaná Metasedimentites (González, 2001) and the intrusive Amagá Stock (Figure 1). Sinifaná depositional and metamorphic ages are not well established, hence relations with the oceanic and continental domains of the northwestern Andes has not been adequately assessed. This work presents zircon U-Pb detrital geochronology of a quartzite that belongs to this unit, constraining the age of deposition and metamorphism, and shedding light on the affinity of this tectonic block with other terranes of the Colombian Andes.

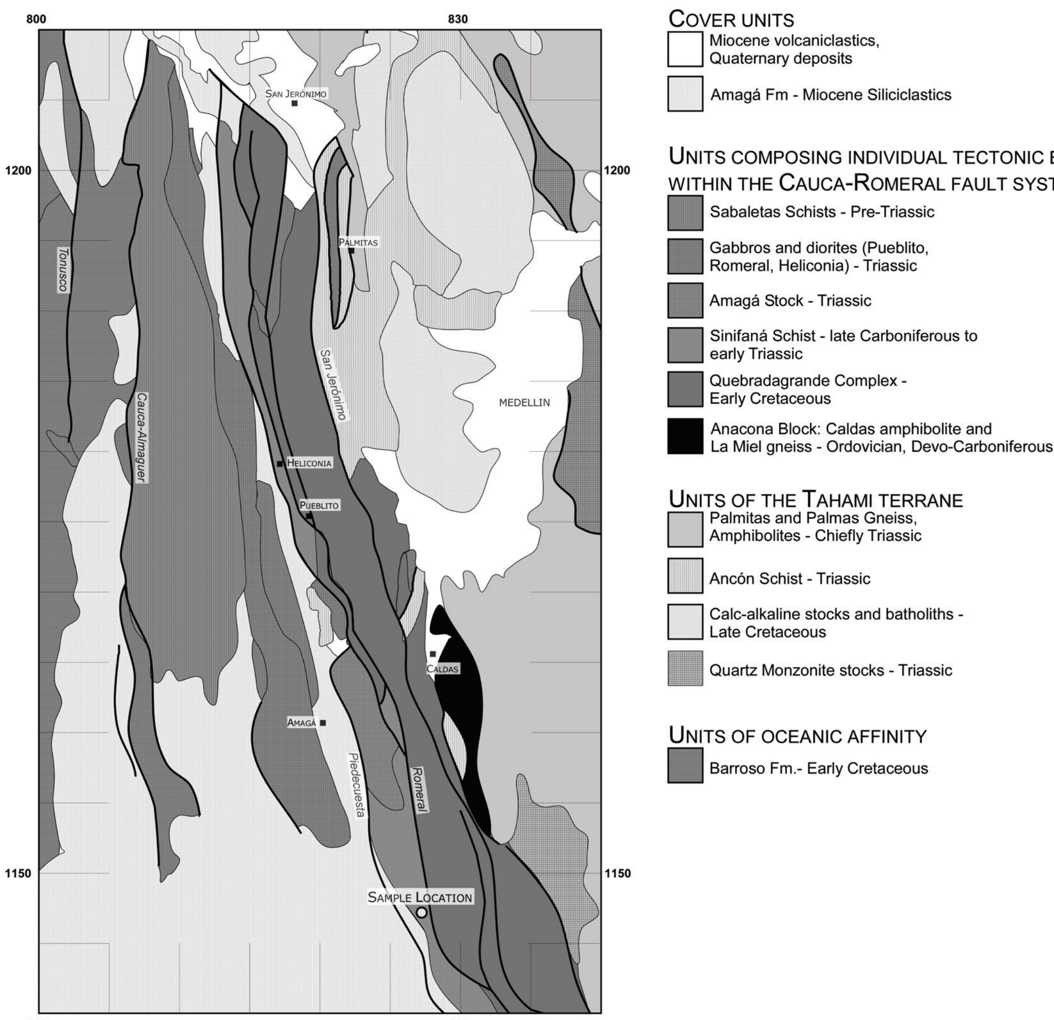


**Figure 1:** Simplified geologic map of the tectonic blocks in the Cauca-Romeral fault system in north-central Colombia, modified from González, 1999. Names of faults in italics. Coordinate system is Colombia West in km.

## 2. GEOLOGIC FRAMEWORK

The Central Cordillera of Colombia is composed chiefly of medium- and high-grade metamorphic rocks (Cajamarca Complex) of Permian to Middle Triassic age that were intruded by small post-tectonic stocks in the Late Triassic (e.g., Restrepo et al., 1991; Vinasco et al., 2006). These rocks were later intruded by voluminous Late Cretaceous plutons of intermediate composition. Of these, the most characteristic is the Antioquia Batholith that has yielded 96-76 Ma ages (Correa et al., 2006; Ibañez-Mejía et al., 2007; Ordoñez et al., 2008; Villagómez et al., 2011). West of these nuclear rocks, a variety of blocks and slivers are bound by the NS-elongated faults of the Cauca-Romeral fault system or megashear (Grosse, 1926). Local faults of the system include the Romeral, San Jerónimo, Cauca, Cauca Este, Sabanalarga, among others (González, 2001). From east to west, the fault-bounded blocks are (a) the medium-grade Anacona terrane metamorphosed during the Devonian (Martens et al., 2011); (b) the Lower Cretaceous volcanosedimentary Quebradagrande Complex (Maya & González, 1995); (c) the Sinifaná metasediments (González, 2001) intruded by the Triassic Amagá granite (Vinasco et al., 2006); (d) the Triassic Pueblito diorite and associated ultramafic and mafic rocks that intrude the Sabaletas Schist (Rodriguez-Jiménez, 2010); (e) the pre-Late Triassic Sabaletas schist (which may contain Cretaceous schists; Giraldo, 2010); and (f) the Barroso complex composed of Cretaceous mafic rocks (González, 2001), which are possibly associated with the Colombia-Caribbean plateau (Kerr et al., 1997). Miocene continental beds of the Amagá Fm (Grosse, 1926) cover many of the above units.

### 2.1. Geologic Characteristics of Sinifaná metasediments and the Amagá stock

The Sinifaná metasedimentites is a N-NNW elongated unit ca. 75 km long and only 3 km where widest. The unit is chiefly composed of intercalations of limy sandstones and siltstones (Bustamante et al., 1999) transformed by very low-grade metamorphism into slate and quartzites. The unit may contain minor occurrences of metacherts and metamafic rocks. Grosse (1926) also reported minor carbonate and mudstone. A small occurrence of phyllite that crops out ca. 10 km north of the main Sinifaná body in the Sucre area has been correlated with it. However, as will be explained below, this correlation is dubious. Primary bedding $S_o$ is still recognizable in contrasting rock types, and incipient $S_1$ schistosity is subparalel to $S_o$. The bounding faults of this unit (Figure 1) are the Romeral (sensu Grosse, 1926) on its eastern flank separating it from the Quebradagrande Complex, and the Piedecuesta and Amagá faults on its western flank separating it from the Amagá Fm and the Pueblito Diorite (Calle et al., 1980). The Amagá granitic stock intruded the Sinifaná metasediments producing a ca. 20 m-wide metamorphic aureole with biotite hornfelses (Giraldo and Toro, 1985; Figure 1). The crystallization age of the Amagá stock is well constrained by SHRIMP U-Pb in zircons which yielded a mean age of 228 ± 5 Ma (Vinasco et al., 2006). The stock has been compared chemically and petrographically to similar intrusions in the Tahamí terrane (e.g., Honda and El Buey stocks; Jaramillo and Ramirez, 1968; Vinasco et al., 2006), for which biotite Ar-Ar cooling dating yielded 219 ± 1 Ma.

The nature of the event that metamorphosed Sinifaná sedimentary rocks is disputed. Whereas Calle et al. (1980) and González (2001) suggested that the metasediments reached greenschist-facies conditions (biotite zone), Bustamante et al. (1999) considered the unit to be anchimetamorphic due to its structural features. Further studies like illite crystallinity or vitrinite reflectance are necessary to address this question. However, available zircon fission-track ages yielding ca. 220 Ma ages (written comm. Gloria Toro) suggest the unit was buried sufficiently deep to have reached temperatures above 250 °C that would anneal fission tracks in zircon. Such a temperature is higher than the 150–200 °C range accepted for anchimetamorphism (e.g., Frey and Kisch, 1987). Therefore in this work we will regard the Sinifaná metasediments as true metamorphic rocks.

### 2.2. Age of Sinifaná Metasediments

The pioneer work of Grosse (1926) described these rocks for the first time assigning a Precambrian or Paleozoic age. González (2001) correlated these rocks with Ordovician low-grade metasediments of La Cristalina and Aquitania which crop out along the eastern flank of the Central Cordillera. In turn, Herrera and Mejía (1989) proposed a Cretaceous age based on the finding of tubular features (Figure 2) that roughly resemble features observed in sedimentary beds of the Western branch of the Colombian Andes. In contrast, we regard the tubes in question to be relics of crinoids (written comm. G.F. Aceñolaza), a type of organism widespread during the late Paleozoic. Bustamante et al. (1999) reported relics of macroflora, which would imply ages younger than late Silurian-lower Devonian (e.g., Edwards, 1979).


**Figure 2:** Photographs of tubular fossils in Sinifaná metasediments, possibly relics of crinoid stems (Adapted from Herrera and Mejía, 1989).

## 3. ANALYTICAL METHODS

Zircons were extracted by standard methods from a quartzite sampled along the Medellín-La Pintada road (Estadero Garibaldi; N 5° 50’ 53.5”, W 75° 34’ 58.4”). Ninety-nine zircons were dated by U-Pb at the Laboratorio de Estudios Isotópicos, Centro de Geociencias, UNAM, by LA-MC-ICPMS (Laser-Ablation Multicollector Inductively-Coupled-Plasma Mass Spectrometry). Laser ablation was conducted using a coherent LPX 200, 193 nm, excimer laser and an optical system equipped with a long working-distance lens, ensuring 50-200 µm focus depth and even-surface energy distribution. Zircons were mounted on 1-inch mounts and 99 grains were ablated in a He-pressurized, double-volume ablation cell to ca. 23 µm diameter and <20 µm depth. The Thermo XII quadrupole ICPMS was tuned to ~ 3,000 cps/ppm $^{238}U$, ThO/Th < 0.5% and $^{238}U/^{232}Th$ ~ 1.05 using NIST 612 glass. During each analysis seventeen species were counted; U, Pb, and Th isotopes were counted for geochronology and Si, P, Ti, Zr, REE’s were counted as petrogenetic indicators or tracers of microscopic inclusions (e.g., monazite, apatite or titanite; e.g. Belousova et al., 2002; Hoskin and Schaltegger, 2003; Allen and Barnes, 2006). Each analysis consisted of monitoring the background for 25 s, counting each species for 30 s while the laser was firing at 5 Hz frequency and ~ 7 J/cm$^2$ energy density on target, and purging for 20 s (about 10 seconds for 5 orders of magnitude washout). Repeated Plešovice standard measurements were used for mass-bias correction, downhole fractionation and time drift (Slama et al., 2008). Three NIST 610 standard glass analyses were used to calculate zircon trace element concentrations. Time-resolved analyses were then reduced offline using an in-house program written in R (Solari and Tanner, 2011). The output was then imported into Excel, where the concordia as well as age-error calculations were obtained using Isoplot v. 3.70 (Ludwig, 2008). During the analytical sessions, the observed uncertainties (1-sigma relative standard deviation) of $^{206}Pb/^{238}U$, $^{207}Pb/^{206}Pb$ and $^{208}Pb/^{232}Th$ on the Plešovice standard were 0.7, 1.2 and 1.3% respectively. These errors were quadratically added to the quoted uncertainties of the measured isotopic ratios of the unknowns. The presence of common Pb was evaluated on Tera-Wasserburg (1972) diagrams of uncorrected isotopic ratios. If needed, common Pb correction was conducted by the algebraic method of Andersen (2002). Throughout the paper $^{206}Pb/^{238}U$ ages are reported for zircons < 800Ma and $^{207}Pb/^{206}Pb$ ages for grains >800 Ma (Table 1).

**Table 1:** U-Pb isotopic ratios and ages.

| Analysis | U (ppm) | Th/U | $^{207}Pb^*/^{206}Pb^*$ | ±1s | $^{207}Pb^*/^{235}U$ | ±1s | $^{206}Pb^*/^{238}U$ | ±1s | Error Corr. | $^{206}Pb^*/^{238}U$ Age (Ma) | ±1s | $^{207}Pb^*/^{235}U$ Age (Ma) | ±1s | $^{207}Pb^*/^{206}Pb^*$ Age (Ma) | ±1s |
|---|---|---|---|---|---|---|---|---|---|---|---|---|---|---|---|
| Zircon_58_076* | 1140 | 0.55 | 0.0584 | 0.0010 | 0.37045 | 0.0084 | 0.04612 | 0.00069 | 0.66 | 291 | 4 | 320 | 6 | 543 | 37 |
| Zircon_78_100 | 217 | 0.63 | 0.0558 | 0.0021 | 0.39298 | 0.01639 | 0.0511 | 0.0004 | 0.28 | 321 | 2 | 337 | 12 | 443 | 84 |
| Zircon_33_046 | 312 | 0.70 | 0.0589 | 0.0020 | 0.41902 | 0.01714 | 0.05158 | 0.0005 | 0.39 | 324 | 3 | 355 | 12 | 564 | 70 |
| Zircon_73_094* | 697 | 0.18 | 0.0597 | 0.0013 | 0.49731 | 0.01176 | 0.0604 | 0.00047 | 0.34 | 378 | 3 | 410 | 8 | 593 | 46 |
| Zircon_44_059 | 297 | 0.41 | 0.0614 | 0.0035 | 0.57813 | 0.03846 | 0.06826 | 0.00129 | 0.49 | 426 | 8 | 463 | 25 | 654 | 122 |
| Zircon_76_098 | 618 | 0.35 | 0.0589 | 0.0018 | 0.58416 | 0.02011 | 0.07199 | 0.00058 | 0.37 | 448 | 4 | 467 | 13 | 562 | 67 |
| Zircon_88_112 | 701 | 0.51 | 0.0563 | 0.0008 | 0.57761 | 0.00902 | 0.07432 | 0.00051 | 0.44 | 462 | 3 | 463 | 6 | 463 | 31 |
| Zircon_56_074* | 408 | 0.26 | 0.0696 | 0.0025 | 0.72313 | 0.03111 | 0.07537 | 0.00108 | 0.56 | 468 | 6 | 553 | 18 | 916 | 74 |
| Zircon_08_016* | 562 | 0.13 | 0.0646 | 0.0011 | 0.68139 | 0.01737 | 0.07688 | 0.00146 | 0.74 | 477 | 9 | 528 | 10 | 761 | 34 |
| Zircon_102_129 | 564 | 0.04 | 0.0627 | 0.0009 | 0.67785 | 0.01117 | 0.07817 | 0.00068 | 0.52 | 485 | 4 | 525 | 7 | 699 | 28 |
| Zircon_34_047* | 119 | 0.76 | 0.0635 | 0.0063 | 0.69128 | 0.07229 | 0.07894 | 0.00083 | 0.12 | 490 | 5 | 534 | 43 | 725 | 199 |
| Zircon_100_126* | 187 | 0.38 | 0.0571 | 0.0027 | 0.62332 | 0.03162 | 0.07922 | 0.00061 | 0.2 | 491 | 4 | 492 | 20 | 494 | 98 |
| Zircon_107_135 | 302 | 0.38 | 0.0629 | 0.0020 | 0.68659 | 0.02734 | 0.07913 | 0.00095 | 0.52 | 491 | 6 | 531 | 16 | 706 | 65 |
| Zircon_17_027 | 514 | 0.35 | 0.0624 | 0.0009 | 0.68632 | 0.01277 | 0.08017 | 0.00088 | 0.59 | 497 | 5 | 531 | 8 | 688 | 30 |
| Zircon_69_089 | 45 | 0.47 | 0.0624 | 0.0021 | 0.68718 | 0.0239 | 0.08024 | 0.00088 | 0.32 | 498 | 5 | 531 | 14 | 689 | 70 |
| Zircon_13_022* | 323 | 0.10 | 0.0571 | 0.0026 | 0.64279 | 0.0321 | 0.0816 | 0.00077 | 0.29 | 506 | 5 | 504 | 20 | 497 | 95 |
| Zircon_12_021 | 523 | 0.21 | 0.0574 | 0.0009 | 0.65396 | 0.01069 | 0.08269 | 0.00054 | 0.4 | 512 | 3 | 511 | 7 | 507 | 31 |
| Zircon_53_070 | 401 | 0.14 | 0.0616 | 0.0009 | 0.70821 | 0.01257 | 0.08373 | 0.0008 | 0.54 | 518 | 5 | 544 | 7 | 660 | 32 |
| Zircon_45_060 | 105 | 0.37 | 0.0595 | 0.0013 | 0.69822 | 0.01687 | 0.08515 | 0.00085 | 0.41 | 527 | 5 | 538 | 10 | 584 | 47 |
| Zircon_11_020 | 615 | 0.27 | 0.0624 | 0.0010 | 0.7372 | 0.01474 | 0.08598 | 0.00103 | 0.6 | 532 | 6 | 561 | 9 | 689 | 32 |
| Zircon_75_096* | 116 | 0.53 | 0.0683 | 0.0089 | 0.81528 | 0.11192 | 0.08657 | 0.00185 | 0.25 | 535 | 11 | 605 | 63 | 878 | 269 |
| Zircon_62_081 | 270 | 0.41 | 0.0596 | 0.0010 | 0.71398 | 0.01338 | 0.08687 | 0.00069 | 0.43 | 537 | 4 | 547 | 8 | 590 | 36 |
| Zircon_20_030 | 309 | 0.02 | 0.0584 | 0.0012 | 0.71479 | 0.01501 | 0.08887 | 0.00057 | 0.3 | 549 | 3 | 548 | 9 | 545 | 41 |
| Zircon_91_116* | 857 | 0.42 | 0.0658 | 0.0020 | 0.8076 | 0.03762 | 0.08896 | 0.00196 | 0.78 | 549 | 12 | 601 | 21 | 801 | 64 |
| Zircon_47_063* | 340 | 0.43 | 0.0661 | 0.0016 | 0.812 | 0.02257 | 0.08907 | 0.00073 | 0.39 | 550 | 4 | 604 | 13 | 810 | 50 |
| Zircon_72_093 | 101 | 0.22 | 0.0619 | 0.0017 | 0.76534 | 0.02218 | 0.08988 | 0.00067 | 0.26 | 555 | 4 | 577 | 13 | 669 | 59 |
| Zircon_90_114 | 91 | 1.04 | 0.0607 | 0.0017 | 0.75063 | 0.02194 | 0.0899 | 0.00076 | 0.29 | 555 | 4 | 569 | 13 | 628 | 60 |
| Zircon_19_029* | 319 | 0.37 | 0.0678 | 0.0018 | 0.84418 | 0.02635 | 0.09025 | 0.00079 | 0.34 | 557 | 5 | 621 | 15 | 864 | 52 |
| Zircon_28_040 | 98 | 0.57 | 0.0578 | 0.0016 | 0.72114 | 0.02137 | 0.09069 | 0.00088 | 0.32 | 560 | 5 | 551 | 13 | 521 | 58 |
| Zircon_26_038 | 254 | 0.41 | 0.0568 | 0.0011 | 0.71228 | 0.01466 | 0.09092 | 0.00072 | 0.38 | 561 | 4 | 546 | 9 | 483 | 39 |
| Zircon_55_072* | 112 | 1.24 | 0.0777 | 0.0056 | 0.98011 | 0.07765 | 0.09151 | 0.00121 | 0.26 | 564 | 7 | 694 | 40 | 1139 | 141 |
| Zircon_61m_080 | 314 | 1.44 | 0.0593 | 0.0011 | 0.7482 | 0.01453 | 0.09148 | 0.00067 | 0.37 | 564 | 4 | 567 | 8 | 578 | 39 |
| Zircon_50_066 | 317 | 0.03 | 0.0601 | 0.0011 | 0.7601 | 0.01468 | 0.09173 | 0.00064 | 0.37 | 566 | 4 | 574 | 8 | 608 | 38 |
| Zircon_29_041 | 181 | 0.34 | 0.0594 | 0.0013 | 0.75342 | 0.01678 | 0.09211 | 0.00068 | 0.33 | 568 | 4 | 570 | 10 | 581 | 43 |
| Zircon_52_069 | 769 | 0.14 | 0.0601 | 0.0008 | 0.76751 | 0.01191 | 0.09259 | 0.00062 | 0.43 | 571 | 4 | 578 | 7 | 607 | 30 |
| Zircon_31_044 | 413 | 0.33 | 0.0600 | 0.0010 | 0.77981 | 0.01411 | 0.09428 | 0.00058 | 0.34 | 581 | 3 | 585 | 8 | 604 | 34 |
| Zircon_64_083 | 789 | 0.24 | 0.0625 | 0.0011 | 0.81306 | 0.01596 | 0.0944 | 0.00056 | 0.37 | 581 | 3 | 604 | 9 | 690 | 37 |
| Zircon_16_026 | 284 | 0.31 | 0.0600 | 0.0011 | 0.78412 | 0.01588 | 0.09477 | 0.00066 | 0.35 | 584 | 4 | 588 | 9 | 605 | 38 |
| Zircon_35_048 | 265 | 0.53 | 0.0629 | 0.0011 | 0.85617 | 0.01644 | 0.09867 | 0.00066 | 0.35 | 607 | 4 | 628 | 9 | 704 | 36 |
| Zircon_21_032* | 109 | 0.16 | 0.0516 | 0.0015 | 0.70736 | 0.02062 | 0.099 | 0.0008 | 0.27 | 609 | 5 | 543 | 12 | 268 | 60 |
| Zircon_27_039 | 221 | 0.01 | 0.0587 | 0.0010 | 0.80406 | 0.01472 | 0.09959 | 0.00068 | 0.37 | 612 | 4 | 599 | 8 | 558 | 35 |
| Zircon_81_104 | 258 | 0.01 | 0.0610 | 0.0015 | 0.84094 | 0.02234 | 0.09954 | 0.0009 | 0.33 | 612 | 5 | 620 | 12 | 641 | 53 |
| Zircon_65_084 | 627 | 0.05 | 0.0595 | 0.0008 | 0.82279 | 0.01241 | 0.10019 | 0.00056 | 0.38 | 616 | 3 | 610 | 7 | 587 | 30 |
| Zircon_10_018 | 74 | 0.31 | 0.0591 | 0.0017 | 0.82001 | 0.02425 | 0.10057 | 0.00096 | 0.31 | 618 | 6 | 608 | 14 | 572 | 57 |
| Zircon_39_053 | 276 | 0.54 | 0.0609 | 0.0011 | 0.85113 | 0.01632 | 0.10115 | 0.00067 | 0.34 | 621 | 4 | 625 | 9 | 637 | 38 |
| Zircon_22_033 | 241 | 0.19 | 0.0603 | 0.0011 | 0.84814 | 0.01626 | 0.10219 | 0.00067 | 0.36 | 627 | 4 | 624 | 9 | 613 | 36 |
| Zircon_89_113 | 415 | 0.27 | 0.0623 | 0.0009 | 0.87931 | 0.01456 | 0.10226 | 0.00072 | 0.43 | 628 | 4 | 641 | 8 | 684 | 32 |
| Zircon_68_088 | 277 | 0.28 | 0.0614 | 0.0010 | 0.86994 | 0.01574 | 0.10269 | 0.00064 | 0.35 | 630 | 4 | 636 | 9 | 653 | 36 |
| Zircon_87_111 | 85 | 0.39 | 0.0603 | 0.0016 | 0.86472 | 0.02409 | 0.1038 | 0.00104 | 0.36 | 637 | 6 | 633 | 13 | 615 | 56 |
| Zircon_101_128* | 120 | 0.50 | 0.0668 | 0.0017 | 0.99502 | 0.03249 | 0.10757 | 0.00226 | 0.64 | 659 | 13 | 701 | 17 | 831 | 49 |
| Zircon_41_056 | 463 | 0.49 | 0.0619 | 0.0010 | 0.9213 | 0.01598 | 0.10779 | 0.00072 | 0.39 | 660 | 4 | 663 | 8 | 672 | 34 |
| Zircon_63_082 | 74 | 0.28 | 0.0609 | 0.0017 | 0.92193 | 0.02672 | 0.10976 | 0.00082 | 0.25 | 671 | 5 | 663 | 14 | 637 | 60 |
| Zircon_92_117 | 541 | 0.58 | 0.0627 | 0.0009 | 0.95635 | 0.0148 | 0.11049 | 0.00073 | 0.42 | 676 | 4 | 681 | 8 | 699 | 30 |
| Zircon_106_134 | 590 | 0.36 | 0.0650 | 0.0013 | 1.01449 | 0.02704 | 0.11316 | 0.00119 | 0.59 | 691 | 7 | 711 | 14 | 775 | 39 |
| Zircon_15_024 | 132 | 0.28 | 0.0641 | 0.0018 | 1.03617 | 0.03568 | 0.11732 | 0.00137 | 0.47 | 715 | 8 | 722 | 18 | 744 | 55 |
| Zircon_09_017 | 360 | 0.21 | 0.0659 | 0.0014 | 1.07803 | 0.03763 | 0.11864 | 0.00221 | 0.75 | 723 | 13 | 743 | 18 | 803 | 42 |
| Zircon_85_108 | 470 | 0.04 | 0.0656 | 0.0010 | 1.09836 | 0.01921 | 0.12141 | 0.0011 | 0.5 | 739 | 6 | 753 | 9 | 794 | 31 |
| Zircon_42_057 | 355 | 0.29 | 0.0631 | 0.0010 | 1.0681 | 0.01857 | 0.12218 | 0.00083 | 0.39 | 743 | 5 | 738 | 9 | 711 | 34 |
| Zircon_84_107 | 458 | 0.08 | 0.0647 | 0.0009 | 1.09273 | 0.0174 | 0.12244 | 0.0009 | 0.48 | 745 | 5 | 750 | 8 | 766 | 29 |
| Zircon_03_010 | 160 | 0.44 | 0.0651 | 0.0012 | 1.1173 | 0.02274 | 0.12438 | 0.00091 | 0.35 | 756 | 5 | 762 | 11 | 777 | 37 |
| Zircon_49_065 | 859 | 0.31 | 0.0688 | 0.0011 | 1.20809 | 0.02446 | 0.12745 | 0.00107 | 0.51 | 773 | 6 | 804 | 11 | 891 | 34 |
| Zircon_07_015 | 183 | 0.04 | 0.0660 | 0.0012 | 1.1851 | 0.02396 | 0.12815 | 0.00118 | 0.45 | 777 | 7 | 794 | 11 | 806 | 35 |
| Zircon_46_062 | 185 | 0.21 | 0.0657 | 0.0011 | 1.1869 | 0.0224 | 0.13023 | 0.00107 | 0.43 | 789 | 6 | 795 | 10 | 798 | 35 |
| Zircon_54_071 | 425 | 0.27 | 0.0649 | 0.0010 | 1.1802 | 0.02081 | 0.13174 | 0.00097 | 0.42 | 798 | 6 | 791 | 10 | 771 | 33 |
| Zircon_70_090 | 658 | 0.29 | 0.0701 | 0.0012 | 1.30713 | 0.02571 | 0.13527 | 0.00094 | 0.46 | 818 | 5 | 849 | 11 | 931 | 34 |
| Zircon_60_078 | 181 | 0.41 | 0.0685 | 0.0012 | 1.2772 | 0.02378 | 0.13548 | 0.00103 | 0.41 | 819 | 6 | 836 | 11 | 883 | 35 |
| Zircon_82_105 | 601 | 0.35 | 0.0652 | 0.0015 | 1.23861 | 0.04084 | 0.13787 | 0.00224 | 0.73 | 833 | 13 | 818 | 19 | 779 | 46 |
| Zircon_18_028 | 498 | 0.33 | 0.0694 | 0.0009 | 1.366 | 0.01962 | 0.14229 | 0.00087 | 0.43 | 858 | 5 | 874 | 8 | 909 | 25 |
| Zircon_67_087* | 140 | 0.76 | 0.0741 | 0.0015 | 1.4657 | 0.04693 | 0.1433 | 0.00358 | 0.78 | 863 | 20 | 916 | 19 | 1044 | 40 |
| Zircon_01 | 98 | 1.10 | 0.0692 | 0.0017 | 1.3644 | 0.03452 | 0.14354 | 0.00115 | 0.32 | 865 | 6 | 874 | 15 | 904 | 46 |
| Zircon_23_034 | 272 | 0.15 | 0.0740 | 0.0013 | 1.54935 | 0.03327 | 0.15192 | 0.00146 | 0.48 | 912 | 8 | 950 | 13 | 1040 | 32 |
| Zircon_86_110 | 562 | 0.13 | 0.0725 | 0.0011 | 1.54586 | 0.02539 | 0.15464 | 0.00102 | 0.42 | 927 | 6 | 949 | 10 | 1000 | 29 |
| Zircon_32_045 | 206 | 0.18 | 0.0720 | 0.0013 | 1.5486 | 0.03189 | 0.15549 | 0.00155 | 0.48 | 932 | 9 | 950 | 13 | 987 | 34 |
| Zircon_83_106 | 281 | 0.37 | 0.0738 | 0.0010 | 1.6858 | 0.02646 | 0.16537 | 0.00117 | 0.46 | 987 | 6 | 1003 | 10 | 1037 | 28 |

| | | | | | | | | | | | | | | | |
|---|---|---|---|---|---|---|---|---|---|---|---|---|---|---|---|
| Zircon_83_106 | 281 | 0.37 | 0.0738 | 0.0010 | 1.6858 | 0.02646 | 0.16537 | 0.00117 | 0.46 | 987 | 6 | 1003 | 10 | 1037 | 28 |
| Zircon_66_086 | 159 | 0.49 | 0.0739 | 0.0014 | 1.7222 | 0.03499 | 0.16881 | 0.00122 | 0.36 | 1006 | 7 | 1017 | 13 | 1040 | 38 |
| Zircon_79_101 | 224 | 0.92 | 0.0758 | 0.0012 | 1.7918 | 0.03182 | 0.17136 | 0.00132 | 0.44 | 1020 | 7 | 1042 | 12 | 1089 | 32 |
| Zircon_14_023 | 85 | 0.45 | 0.0743 | 0.0015 | 1.7848 | 0.03819 | 0.17261 | 0.00131 | 0.35 | 1026 | 7 | 1040 | 14 | 1050 | 38 |
| Zircon_02_009 | 94 | 0.73 | 0.0731 | 0.0016 | 1.8018 | 0.04128 | 0.17889 | 0.00114 | 0.28 | 1061 | 6 | 1046 | 15 | 1017 | 42 |
| Zircon_25_036 | 295 | 0.22 | 0.0767 | 0.0011 | 1.90249 | 0.0351 | 0.17991 | 0.00136 | 0.46 | 1066 | 7 | 1082 | 12 | 1113 | 27 |
| Zircon_24_035 | 51 | 0.59 | 0.0731 | 0.0017 | 1.8169 | 0.04632 | 0.18076 | 0.00199 | 0.43 | 1071 | 11 | 1052 | 17 | 1015 | 44 |
| Zircon_40_054 | 379 | 0.77 | 0.0779 | 0.0010 | 2.005 | 0.02951 | 0.18661 | 0.00129 | 0.47 | 1103 | 7 | 1117 | 10 | 1143 | 26 |
| Zircon_59_077 | 207 | 0.49 | 0.0824 | 0.0012 | 2.1956 | 0.03682 | 0.19286 | 0.00145 | 0.44 | 1137 | 8 | 1180 | 12 | 1255 | 29 |
| Zircon_57_075 | 591 | 0.57 | 0.0817 | 0.0011 | 2.2602 | 0.03208 | 0.20056 | 0.00114 | 0.4 | 1178 | 6 | 1200 | 10 | 1237 | 25 |
| Zircon_36_050 | 240 | 0.68 | 0.0887 | 0.0014 | 2.9838 | 0.05311 | 0.24405 | 0.0019 | 0.44 | 1408 | 10 | 1403 | 14 | 1397 | 29 |
| Zircon_30_042 | 311 | 0.51 | 0.0962 | 0.0013 | 3.6771 | 0.05234 | 0.27682 | 0.00161 | 0.41 | 1575 | 8 | 1566 | 11 | 1552 | 23 |
| Zircon_71_092 | 221 | 0.27 | 0.1457 | 0.0019 | 8.5026 | 0.12396 | 0.42243 | 0.00279 | 0.46 | 2272 | 13 | 2286 | 13 | 2296 | 22 |
| Zircon_51_068 | 85 | 0.49 | 0.1542 | 0.0022 | 9.0212 | 0.14041 | 0.42343 | 0.00288 | 0.44 | 2276 | 13 | 2340 | 14 | 2393 | 24 |
| Zircon_04_011* | 270 | 0.33 | 0.0849 | 0.0014 | 2.06532 | 0.04184 | 0.17651 | 0.00126 | 0.41 | | | | | | |
| Zircon_05_012* | 440 | 0.58 | 0.0798 | 0.0018 | 1.51752 | 0.04128 | 0.13801 | 0.0011 | 0.48 | | | | | | |
| Zircon_06_014* | 225 | 0.30 | 0.0871 | 0.0013 | 1.9201 | 0.03688 | 0.15428 | 0.00185 | 0.62 | | | | | | |
| Zircon_103_130* | 416 | 0.40 | 0.1170 | 0.0015 | 5.0764 | 0.08226 | 0.31477 | 0.00194 | 0.42 | | | | | | |
| Zircon_104_131* | 375 | 0.15 | 0.1118 | 0.0017 | 1.95529 | 0.03953 | 0.12689 | 0.00124 | 0.56 | | | | | | |
| Zircon_105_132* | 233 | 0.31 | 0.1420 | 0.0019 | 5.53788 | 0.10026 | 0.28284 | 0.00262 | 0.56 | | | | | | |
| Zircon_108_136* | 130 | 0.55 | 0.0871 | 0.0050 | 1.6371 | 0.1124 | 0.13633 | 0.00263 | 0.43 | | | | | | |
| Zircon_109_137* | 13 | 1.90 | 0.0828 | 0.0072 | 2.26719 | 0.23371 | 0.19849 | 0.00411 | 0.33 | | | | | | |
| Zircon_112_141* | 680 | 0.04 | 0.1293 | 0.0017 | 2.33614 | 0.05029 | 0.131 | 0.00197 | 0.73 | | | | | | |
| Zircon_37_051* | 371 | 0.27 | 0.1055 | 0.0020 | 3.7172 | 0.11672 | 0.24799 | 0.0062 | 0.8 | | | | | | |
| Zircon_38_052* | 855 | 0.41 | 0.0808 | 0.0023 | 1.43991 | 0.06034 | 0.12927 | 0.00256 | 0.79 | | | | | | |
| Zircon_74_095* | 1290 | 0.64 | 0.0877 | 0.0015 | 1.3984 | 0.16948 | 0.11656 | 0.01399 | 0.99 | | | | | | |

*Analyses included in probability density estimation.

## 4. RESULTS

In thin section the siliciclastic character of the dated Sinifaná rock is well preserved. The rock exhibits subangular to subrounded detrital quartz grains and metamorphic rock fragments bearing fine white mica. Additionally, the sample shows incipient schistosity defined by phyllosilicates and by discrete cleavage domains of insoluble opaques (Figure 3). These features are characteristic of pressure solution and the initial stages of metamorphic recrystallization, chiefly of the rock's matrix.

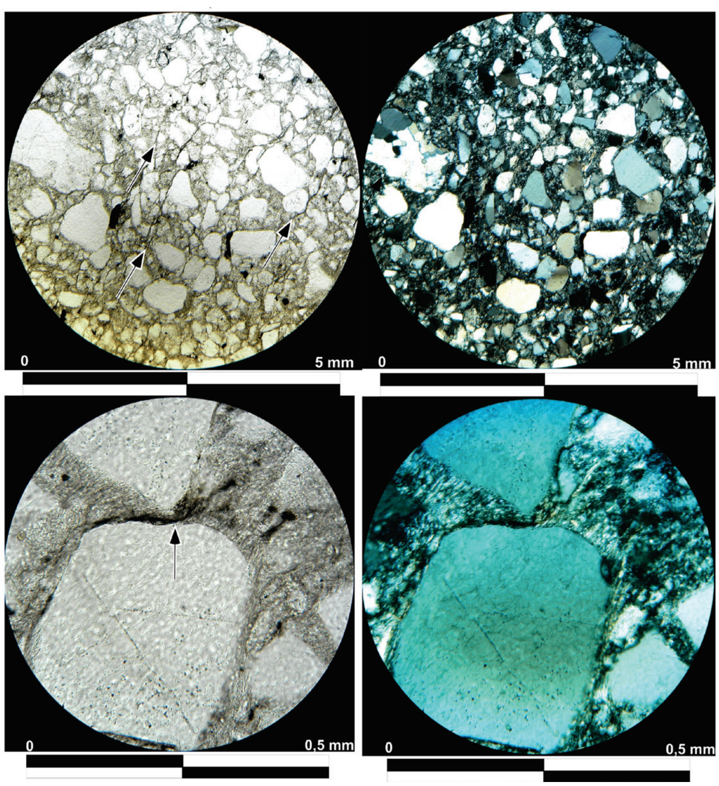


**Figure 3.** Thin section from a meta-arenite of the Sinifaná metasediments.

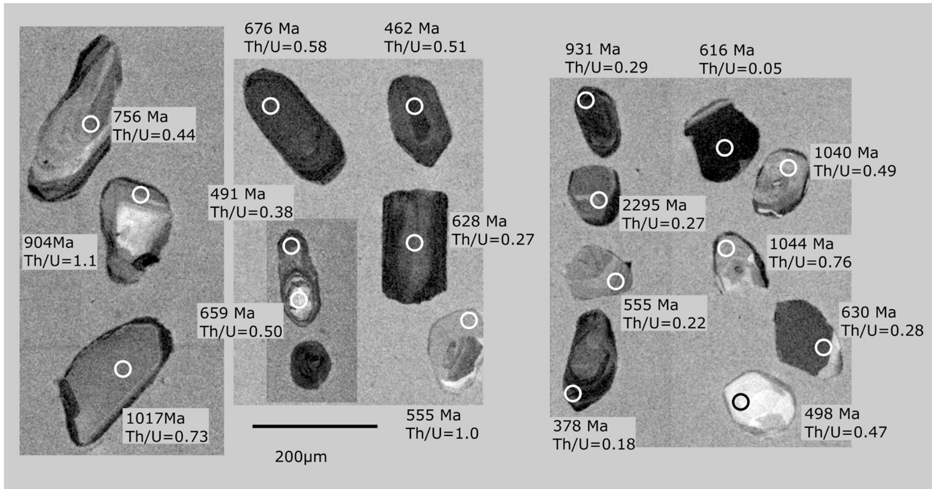


**Figure 4:** Examples of CL images of the dated zircon. Circles represent dated spots.

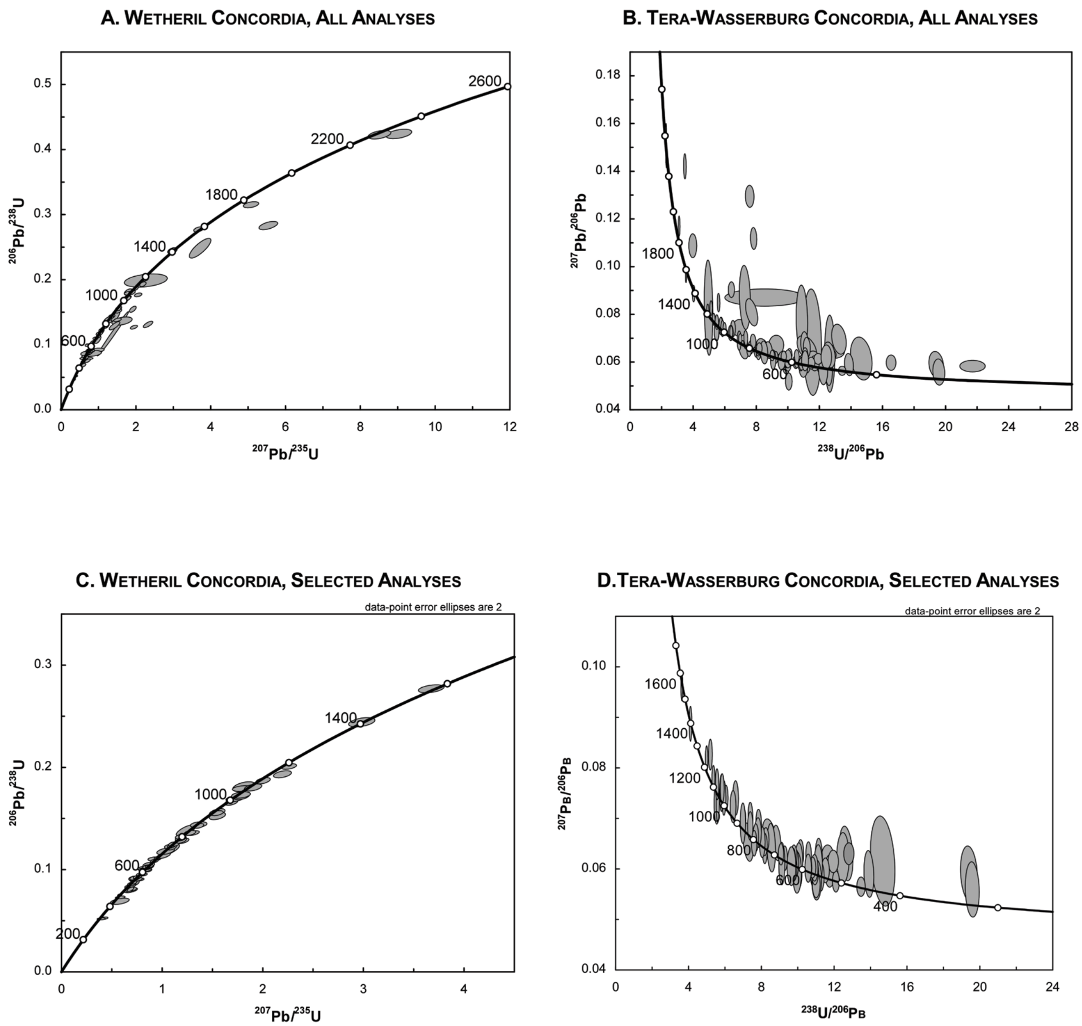


**Figure 5:** Concordia diagram of dated zircons. (A) Wetherill concordia and (B) Tera-Wasserburg concordia of all 99 analyses. (C) Wetherill concordia and (D) Tera-Wasserburg concordia of 72 analyses selected for probability density estimation; two Paleoproterozoic analyses not shown.

 Boletín Ciencias de la Tierra, Nro. 32, pp. 99-110. Medellín, diciembre de 2012. ISSN 012-3630

The dated zircons are anhedral, equant to short prismatic, very rounded, features that are consistent with sedimentary transport. CL images revealed a variety of textures (Figure 4): sector zoning is common, concentric less so, many are dark, and a few show thin rims. Wetherill and Tera-Wasserburg concordia diagrams of the 99 analysed spots are shown in Figure 5A-B. Figure 5C-D shows similar diagrams for the 72 analyses that were regarded suitable for the probability density estimations (Figure 6). The most abundant zircon populations have ages in the 640–500 Ma range with probability peaks at 620 Ma, 565 Ma, and 515 Ma. These ages correspond to the Pan African-Brasiliano orogeny. Other minor age groups include 800–720 Ma and ca. 1040 Ma. The former is a relatively uncommon group in detrital populations, whereas the latter is typical Grenville. In the few grains in which it was feasible to date both the core and the rim, the later yielded chiefly early Paleozoic ages (example in Figure 4).

The youngest age group is ca. 325–320 Ma old (n=2) and the youngest grain is ca. 291 Ma, implying post late Carboniferous deposition of Sinifaná siliciclastics. The oldest zircons in the sample are ca. 2.3-2.4 Ga (n=2). Most zircons have Th/U>2 but, interestingly, some of the analyses that yielded ages in the 800–460 Ma range have Th/U<0.05. Although not a very robust indicator (e.g., Hoskin & Schaltegger, 2003; Harley et al., 2007), this elemental ratio suggests that some of the Pan-African-Brasiliano zircons were produced by metamorphism (Figure 7).

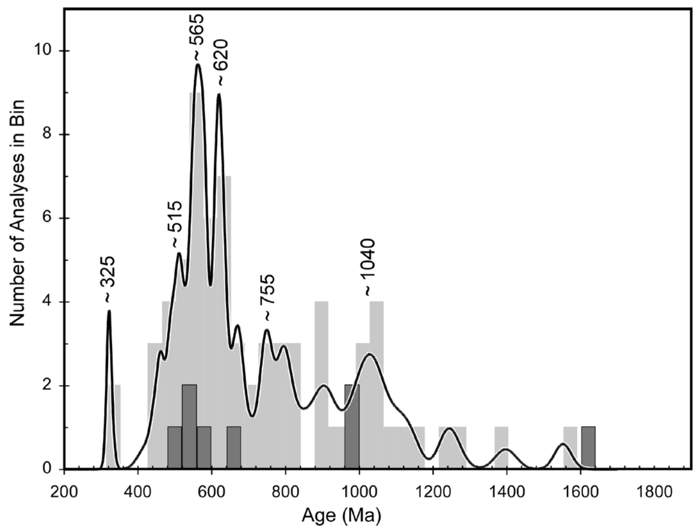


**Figure 6:** Histogram and probability density model of Sinifaná detrital U-Pb ages (light gray bins) showing ages of main populations. For contrast, inherited U-Pb ages of Amagá stock are shown as dark gray bins.

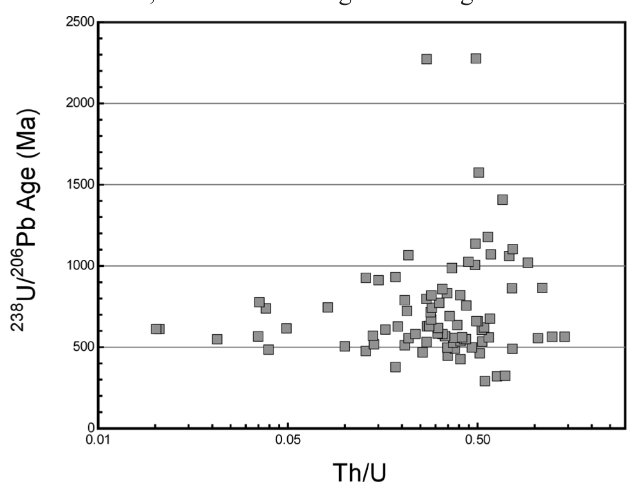


**Figure 7:** Th/U ratio vs. age of analyzed zircons. Notice group of Pan-African zircons with Th/U < 0.05.

## 5. DISCUSSION AND CONCLUSION

The chief detrital zircon population in the Sinifaná quartzite is 650–500 Ma, ages characteristic of the Brasiliano-Pan African orogeny. This feature strongly suggests affinity with Gondwanan terranes (e.g., Veevers, 2003). An analogous age range was found in the main inherited-zircon populations of the undeformed Amagá stock and the high-grade rocks in Las Palmas (Vinasco et al., 2006; Martens et al., 2011). This affinity opens an interesting possibility: Sinifaná metasediments could have been derived from sources similar and related to those of metasedimentary rocks that underwent high-grade metamorphism and partial melting in the Cajamarca complex. Based on the similarities in sedimentary provenance and magmatic rocks, we propose that the Sinifaná-Amagá block within the Cauca-Romeral fault system may have formed as a para-autochthonous block from the Tahamí terrane. We hypothesize that previous to the Triassic, the Tahamí terrane was covered by one or several siliciclastic basins that incorporated chiefly Gondwanan zircons of Ediacaran–Cambrian age. These sedimentary units included both the protoliths of Las Palmas as well as Sinifaná. A regional Triassic tectonomagmatic event reworked Tahamí's supracrustal cover to various degrees, producing low-grade metasedimentary rocks (e.g., Sinifaná) as well as high-grade rocks in the core of the orogen (e.g., Las Palmas). Metamorphic rims yielding 235–245 Ma are ubiquitous in Las Palmas constraining the age of metamorphism. Although metamorphic rims are absent in Sinifaná, a reflection of very-low-grade metamorphism not being capable of producing zircon recrystallization, the age constraints for Sinifaná presented above imply an age range consistent with Early or Middle Triassic metamorphism.

Both metamorphic units were intruded by similar post-tectonic stocks in the Late Triassic (e.g., La Honda, El Buey, Amagá). After Late Cretaceous closure of the ocean between the Caribbean oceanic plateau, the Quebradagrande arc, and the continental margin, the Cauca-Romeral fault system produced a series of NS-elongated tectonic slivers including pieces of the continental margin. These were juxtaposed and mixed as deformation proceeded along the anastomosing faults. We therefore conclude that the current relative positions of blocks in the fault system was significantly altered and does not reflect the original positions of the geologic environments where each of the blocks was generated.

Although paleolatitudes are very hard to constrain, we envision the Sinifaná block braking away from a position south of its current location and possibly migrating northward (Toussaint, 1996; Bayona et al., 2006; Pindell and Kennan, 2009). The age of tectonic transport is ultimately constrained by the age of the Early Cretaceous Quebradagrande complex, which is located in between Tahamí and Sinifaná (Fig. 1).

Finally, a comment on the detrital geochronology of a sample of what is supposedly the northern extension of the Sinifaná unit in the Sucre area. The zircon U-Pb ages contain a significant Permo-Triassic contribution (ca. 30%; Vinasco et al., 2011). Inasmuch as these ages are completely absent in the sample analysed in this study, we conclude that metasedimentary rocks near Sucre were part of a different, younger basin. Furthermore, as discussed above, the Triassic Amagá Stock intrudes the Sinifaná Metasedimentites, so a post-Triassic sedimentary or metamorphic record seems very unlikely.

## ACKNOWLEDGMENTS

We express gratitude to Carlos Ortega Obregón at CGEO-UNAM for formidable assistance during the U-Pb analytical session. César Vinasco is thanked for editorial handling and fruitful discussions on the origin of the Sinifaná block.

## REFERENCES

[1] Allen,C.M., Barnes,C.G., 2006. Ages and some cryptic sources of Mesozoic plutonic rocks in the Klamath Mountains, California and Oregon,in Snoke, A.W., Barnes, C.G. (eds.), Geological studies in the Klamath Mountains province, California and Oregon: A volume in honor of William P. Irwin: Boulder, Colorado, Geological Society of America, Special Paper 410, 223-245.

[2] Andersen, T., 2002. Correction of common lead in U–Pb analyses that do not report 204Pb: Chemical Geology, v. 192, p. 59-79.

[3] Bayona, G., Rapalini, A., Constanzo-Alvarez, V.l., 2006. Paleomagnetism in Mesozoic rocks of the Northern Andes and its Implications in Mesozoic Tectonics of Northwestern South America Earth Planets Space, 58, 1255–1272.

[4] Belousova, E.A.; Griffin, W.L.; O'Reilly, S.Y.; Fisher, N.I. 2002. Igneous zircon: trace element composition as an indicator of source rock type. Contrib Mineral Petrol. 143: 602–622.

[5] Bustamante, A., Cardona, A., Durán, C.T. 1999. Estratigrafía y Petrogénesis de las Sedimentitas Paleozóicas en el Flanco Occidental de la Cordillera Central, Departamento de Antioquia. Trabajo de grado Universidad Eafit, Medellín, pp. 1-102.

[6] Calle, B., González, H., De La Peña, R., Escorce, E., Durango, J., 1980. Plancha 166- Jericó, escala 1:100.000. Ingeominas, Bogotá.

[7] Correa M., A.M., Pimentel, M., Restrepo, J.J., Nilson, A., Ordoñez, O., Martens, U., Laux, J.E., Junges, S., 2006, U-Pb zircon ages and Nd-Sr isotopes of Altavista Stock and the San Diego Gabbro: New insights of Cretaceous arc magmatism in the Colombian Andes. V SSAGI, Punta del Este, Uruguay.

[8] Edwards, D., 1979. The early history of vascular plants based on late Silurian and early Devonian floras of the British Isles. Geological Society, London, Special Publications 8.

[9] Frey, M., Kisch, H.J.1987. Scope of subject. In: Frey, M., editor. Low temperature metamorphism, New York: Blackie & Sons, p. 1-8.

[10] Giraldo, M.I. 2010. Esquema geodinámico de la parte noroccidental de la Cordillera Central de Colombia. Trabajo de grado de maestría, Universidad Nacional Sede Medellín, pp. 1-146

[11] Giraldo, B.N., Toro L.M. 1985. Cartografía detallada del Stock de Amagá y sus rocas encajantes. Proyecto de grado. Universidad Nacional Sede Medellín, pp 1-200.

[12] González, H. 1999. Geología del Departamento de Antioquia 1:400.000, Ingeominas, Bogotá.

[13] González, H. 2001. Memoria explicativa del mapa de Antioquia 1:400.000, Ingeominas, Bogotá, pp 1-240.

[14] Grosse, E., 1926. El Terciario Carbonífero de Antioquia. Ed. Reimer, Berlín, pp 1-361.

[15] Harley, S.L., Kelly, N.M., Möller, A. 2007. Zircon behaviour and the thermal histories of mountain chains. Elements 3, pp. 25 – 30.

[16] Herrera, H.M., Mejía, J.C., 1989. Estudio geomorfológico y estructural de la Cuenca del Río Poblanco. Trabajo de grado. Universidad Nacional de Colombia Sede Medellín.

[17] Hoskin, P.W.O. and Schaltegger, U., 2003. The composition of zircon and igneous and metamorphic petrogenesis. In: Zircon, J.M. Hanchar & W.O. Hoskin (eds.). Reviews in Mineralogy and Geochemistry 53, pp. 27–62.

[18] Ibañez-Mejia, M., Tassinari, C.C.G., Jaramillo-Mejia, J.M., 2007. U–Pb zircon ages of the "Antioquian Batholith": geochronological constraints of Late Cretaceous magmatism in the Central Andes of Colombia. 11th Colombian Geological Congress, extended abstracts. 11 p.

[19] Jaramillo, Iván & Ramírez, Octavio, 1968. El Cretáceo de Abejorral, Antioquia. Tesis de grado, Universidad Nacional, Fac. Minas, Medellín, pp 1-63.

[20] Kerr, A.C., Marriner, G. F., Tarney, J., Nivia, A., Saunders, A. D., Thirlwall, M. F. & Sinton, C., 1997. Cretaceous Basaltic Terranes in Western Colombia: Elemental, Chronological and Sr-Nd Isotopic Constraints on Petrogenesis. Journal of Petrology, 38, 677-702.

[21] Ludwig, K., 2008, Manual for Isoplot 3.7: Berkeley Geochronology Center Special Publication No. 4, rev. August 26, p. 77.

[22] Martens, U., Restrepo, J.J.; Ordoñez-Carmona, O. 2011. In-situ U/Pb geochronology reveals distinct cristal domains in the western flank of Colombia´s Central Cordillera. Memorias XIV Congreso Latinoamericano de Geología, p. 322, Medellín, Colombia.

[23] Maya, M., González, H., 1995. Unidades litodémicas en la Cordillera Central de Colombia. Boletín Geológico, Ingeominas, Vol. 35(2-3), pp. 43-57, Bogotá.

[24] Ordoñez, O., Pimentel, M., Laux, J.H., 2008. Edades U-Pb del Batolito Antioqueño. Bol. Ciencias de la Tierra, Universidad Nacional, Sede Medellín, p- 129-130.

[25] James Pindell, J, Kennan, L., 2009. Tectonic evolution of the Gulf of Mexico, Caribbean and northern South America in the mantle reference frame: an update. In James, K., Lorente, M. A. & Pindell, J. (eds), The geology and evolution of the region between North and South America, Geological Society, London, Special Publications, v. 328, pp. 1-55.

[26] Restrepo, J.J., Toussaint, J.F., González, H., Cordani, U., Kawashita, K., Linares, E., Parica, C., 1991. Precisiones geocronológicas sobre el occidente colombiano. In: Simposio sobre magmatismo andino y su marco tectónico. Memorias, Tomo I., pp. 1-22, Manizales, Colombia.

[27] Restrepo, J.J., Ordóñez-Carmona, O., Armstrong, R., Marcio M. Pimentel, Marcio M., 2011 Triassic metamorphism in the northern part of the Tahamí Terrane of the central cordillera of Colombia. Journal of South American Earth Sciences 32, 497-507.

[28] Rodriguez-Jiménez, J.V., 2010. Fábrica y emplazamiento de la Diorita de Pueblito, NW Cordillera Central de Colombia: análisis de fábrica magnética y mineral. Trabajo de grado de maestría, Universidad Nacional Sede Medellín, pp. 1-60.

[29] Sláma, J., Kosler, J., Condon, D., Crowley, J., Gerdes, A., Hanchar, J., Horstwood, M., Morris, G., Nas-dala, L., Norberg, N., Schaltagger, U., Schoene, B., Tubrett, M.N., and Whitehouse, M.J., 2008. Plešovice zircon — A new natural reference material for U–Pb and Hf isotopic microanalysis: Chemical Geology, v. 249, p. 1-35.

[30] Solari, L.A., and Tanner, M., 2011. UPb. age, a fast data reduction script for LA-ICP-MS U-Pb geo-chronology: Revista Mexicana de Ciencias Geológicas, v. 28, n. 1, 83-91.

[31] Tera, F. and Wasserburg, G.J., 1972. U–Th–Pb systematics in three Apollo 14 basalts and the problem of initial Pb in lunar rocks: Earth and Planetary Science letters, v. 14, p. 281–304.

[32] Toussaint, J.F., 1996. Evolución geológica de Colombia, Tomo 3 Cretácico. Universidad Nacional de Colombia, Sede Medellín, pp 1-277.

[33] Veevers, J.J., 2003. Pan-African is Pan-Gondwanaland: oblique convergence drives rotation during 650-500 Ma assembly. Geology 31 (6), pp 501-504.

[34] Villagómez, D., Spikings, R. Magna, T. Kammer, A. Winkler, W Beltrán, A., 2011. Geochronology, geochemistry and tectonic evolution of the Western and Central cordilleras of Colombia. Lithos 125 pp. 875–896.

[35] Vinasco, C.J., Cordani, U.G., González, H., Weber, M., Peláez, C., 2006. Geochronological, isotopic, and geochemical data from Permo-Triassic granitic gneisses and granitoids of the Colombian Central Andes. J. South Am. Earth Sci. 21 (4), pp. 355-371.

[36] Vinasco, C.J., Weber, M., Cardona, A., Areiza, M., Restrepo, S., Pindell, J., Pardo, A., Toro, L.M., Lara, M., 2011. Geological transect through an accretionary margin, Western Colombia. Field trip September 3-5, 2011, IGCP Project 546 “Subduction zones of the Caribbean”, Medellín.